



**HAL**  
open science

# Influence of uncertainties on the positioning of cable-driven parallel robots

Jean-Pierre Merlet

► **To cite this version:**

Jean-Pierre Merlet. Influence of uncertainties on the positioning of cable-driven parallel robots. IROS 2019 - IEEE/RSJ International Conference on Intelligent Robots and Systems, Nov 2019, Macau, China. hal-02426402

**HAL Id: hal-02426402**

**<https://inria.hal.science/hal-02426402v1>**

Submitted on 2 Jan 2020

**HAL** is a multi-disciplinary open access archive for the deposit and dissemination of scientific research documents, whether they are published or not. The documents may come from teaching and research institutions in France or abroad, or from public or private research centers.

L'archive ouverte pluridisciplinaire **HAL**, est destinée au dépôt et à la diffusion de documents scientifiques de niveau recherche, publiés ou non, émanant des établissements d'enseignement et de recherche français ou étrangers, des laboratoires publics ou privés.

# Influence of uncertainties on the positioning of cable-driven parallel robots

J-P. Merlet<sup>1</sup>

**Abstract**—Positioning accuracy of cable-driven parallel robots is influenced by many factors such as geometry, actuator sensor accuracy and disturbances in the applied wrench. Another uncertainty source is the elasticity of the cables. While the influence of many factors may be decreased by calibration and/or sensor fusion, elasticity parameters are difficult to estimate and their effect on the positioning errors has yet to be determined. In this paper we consider a generic cable model that include cable elasticity and the effect of cable weight and we propose a generic algorithm that allows one to safely calculate the minimum and maximum of the positioning error at a given pose when the elasticity parameters are constrained to lie within some given bounds. The algorithm is designed for being able to manage the effect of different uncertainties sources and we compare the influence of elasticity versus the effect of uncertainties in the cable lengths.

**Index terms:** parallel robot cable-driven parallel robot, accuracy, uncertainties

## I. INTRODUCTION

We consider a variant of parallel robots, namely cable-driven parallel robots (CDPR), in which the rigid legs of parallel robots are substituted by coilable/uncoilable cables. Cables are coiled on a winch whose cable output is a fixed point  $A$ , while the cable extremity is attached to the end-effector at point  $B$  (figure 1). For CDPR any kinematic problem involves also cable tensions as cables can exert only a pulling action so that the name *kineto-static* is often used. Consequently kinematic modeling of CDPR is highly dependent upon the statics modeling of cable. In a vast majority of works cables are assumed to be *ideal* i.e. the cable shape is the straight line between  $A$  and  $B$  and its length  $L_0$  is independent from the cable tension  $\tau$ , figure 1. But a more realistic modeling is to consider that there is elasticity in the cable and not to ignore the cable weight, both factors having an influence on the kineto-static behavior of the robot.

Elasticity behavior is usually based on the knowledge of the Young modulus of the cable material. However measuring this parameter is not easy and this parameter is time-varying because of the cable wear. Managing this type of uncertainties for CDPR is not a well-studied topic. Researchers rely on robust control [1],[2], the effect of uncertain wrench applied on the platform [3] or on the cable lengths [4] or the use of additional sensors for reducing the effect of the uncertainties [5] or even to get rid of any model by using a vision system [6]. Still is lacking an analysis of the consequences of uncertainties on the elasticity parameters.

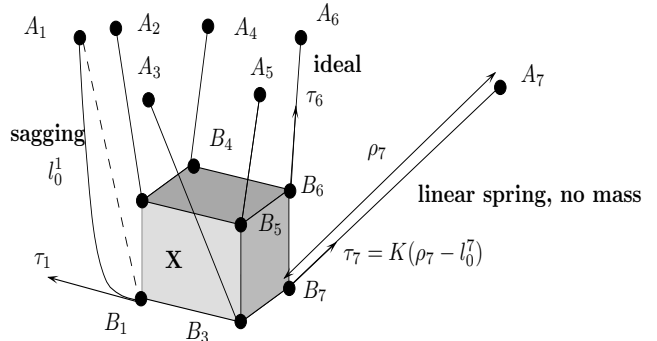


Fig. 1. A CDPR and various cable model

The purpose of this paper is to consider a realistic cable model and to determine the minimum and maximum positioning error first around a nominal pose that is a solution of the direct kinematics for fixed cable lengths, assuming that the Young modulus of the cable material is uncertain but is constrained to lie within known intervals.

## II. CABLE MODEL

In this paper we will use the Irvine sagging cable model that is valid for elastic and deformable cable with mass [7] and that has been shown to be in very good agreement with experimental results [8] (note that the attribution of this model to Irvine is uncertain). This model is widely used for medium-size and large CDPR [9], [10], [11], [12] and we have shown that it is interesting to use for the exploitation of additional sensors beside the cable lengths with the purpose of improving the accuracy of CDPR [13]. Beside its agreement with experimental data, the motivation for using this cable model is that it allows to include in a compact way both the elasticity of the cable and the effect of the cable weight, while lumped-mass model [14] have a much larger set of parameters. Another interest of the Irvine model is that it leads to the ideal cable model if  $E \rightarrow \infty, \mu \rightarrow 0$ , thereby allowing the use of a continuation approach for managing kinematics problems [15]. Much complex cable models exist [16], [17], [18] but have not yet been used for CDPR..

The Irvine model assumes that the cable lies in a vertical plane and is a 2D model (figure 2). In this plane a frame is defined with origin the upper attachment point of the cable  $A(0,0)$  and horizontal and vertical axis  $x_r, z_r$ . The cable lower attachment point  $B$  has as coordinates  $(x^r \geq 0, z^r <$

<sup>1</sup>HEPHAISTOS project, INRIA, France  
Jean-Pierre.Merlet@inria.fr

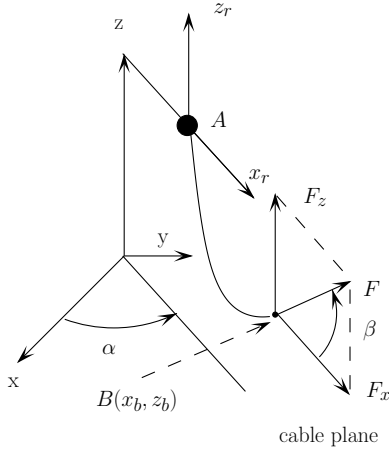


Fig. 2. Notation for a sagging cable

0). Vertical and horizontal forces  $F_z, F_x > 0$  are exerted on the cable at point  $B_i$ . For a cable with length at rest  $L_0$  the coordinates of  $B$  are given by [7]:

$$\begin{aligned} x^r &= F_x \left( \frac{L_0}{EA_0} + \frac{\sinh^{-1}(F_z) - \sinh^{-1}(F_z - \mu g L_0 / F_x)}{\mu g} \right) \\ z^r &= \frac{F_z}{EA_0} - \frac{\mu g L_0^2}{2} + \frac{\sqrt{F_x^2 + F_z^2} - \sqrt{F_x^2 + (F_z - \mu g L_0)^2}}{\mu g} \end{aligned} \quad (2)$$

where  $E$  is the Young modulus,  $A_0$  is the cable cross-section area, and  $\mu$  is the cable linear density. CDPR uses a set of cables whose Young modulus  $E_i$  (for cable  $i$ ) will be considered to be independent but also constrained to lie in a known range  $[E_i, \bar{E}_i]$ . While  $\mu$  may be estimated accurately, the Young modulus is more difficult to measure and will change over time because of the wear of the cable. But the influence of these changes on the positioning accuracy of a CDPR has yet to be determined. Hence one objective of this paper

### III. KINEMATICS AND STATICS

We will consider the pose  $\mathbf{X}$  of a CDPR with  $n$  cables obtained for given values for the cable lengths at rest  $\{L_0^1, L_0^2, \dots, L_0^n\}$ , so that  $\mathbf{X}$  is a solution of the *direct kinematic* problem. We consider a CDPR with  $n$  cables, cable  $i$  being attached on the platform at point  $B_i$  while the output point of the cable at the winch will be denoted by  $A_i$ .

We define a reference frame  $(O, \mathbf{x}, \mathbf{y}, \mathbf{z})$  with a vertical upward  $\mathbf{z}$  axis and the components of the vector  $\mathbf{OA}_i$  in this frame are assumed to be known. We also define a mobile frame for the platform  $(C, \mathbf{x}_m, \mathbf{y}_m, \mathbf{z}_m)$ , where  $C$  is the center of mass of the platform, and we assume that the components of the vector  $\mathbf{CB}_{i_m}$  in this frame are known. A pose of the CDPR will be defined by the coordinates of  $C$  in the reference frame and by a rotation matrix  $\mathcal{R}$  that transform a vector from the mobile frame to the reference frame. With this notation we have in the reference frame

$$\mathbf{A}_i \mathbf{B}_i = \mathbf{OC} + \mathbf{CB}_i - \mathbf{OA}_i = \mathbf{OC} + \mathcal{R} \mathbf{CB}_{i_m} - \mathbf{OA}_i$$

For using the Irvine equation we need to obtain  $\mathbf{A}_i \mathbf{B}_i$  in the cable frame. For that purpose we have to use a unique rotation matrix  $\mathcal{R}_i$  that describe a rotation of angle  $\alpha$  around the vertical and such that  $\mathcal{R}_i \mathbf{A}_i \mathbf{B}_i = (x_i^r > 0, 0, z_i^r)^T$ , where  $z_i^r$  is the  $z$  component of  $\mathbf{A}_i \mathbf{B}_i$ . We have therefore a constraint  $A_\alpha = 0$  on  $\alpha$  that must be such that the second component of  $\mathcal{R}_i \mathbf{A}_i \mathbf{B}_i$  must be 0. The unknowns of the direct kinematics are therefore the  $2n$   $F_x^i, F_z^i$ , the  $n$   $\alpha^i$  and the components of  $\mathbf{X}$  (6 for a 6 d.o.f robot and 3 for a planar robot) for a total of  $3n + 6$  unknowns ( $3n + 3$  for a planar robot).

As for the constraints we the  $2n$  Irvine equations for  $x_i^r, z_i^r$  and the  $n$  constraints  $A_\alpha^i = 0$ . But we have to consider that the system is in a mechanical equilibrium. If  $(F_{x_i} > 0, F_{z_i})$  are the components of the force that is applied by the platform on the cable at  $B_i$  in its plane, then the force exerted by the cable on the platform in the reference frame is  $\mathbf{F}_a^i = \mathcal{R}_i^T (F_{x_i} > 0, F_{z_i})^T$ . We assume that the platform is subjected only to gravity which exert a vertical force  $\mathcal{F}$  and no torque around the platform center of mass  $C$ . Hence the mechanical equilibrium imposes

$$\sum_{j=1}^{j=n} \mathbf{F}_a^j + \mathcal{F} = \mathbf{0} \quad \sum_{j=1}^{j=n} \mathbf{CB}_i \times \mathbf{F}_a^j = \mathbf{0} \quad (3)$$

This provides 6 additional constraints (3 for a planar robot) so that we have  $3n + 6$  constraints ( $3n + 3$  for a planar robot). Consequently solving the direct kinematics requires to solve a square system  $\mathcal{H}(\mathbf{X}) = 0$ , which will admit, in general, a finite number of solutions.

### IV. EXTREMAL POSITIONING ERROR AROUND A POSE

We assume that the CDPR should be in a nominal pose  $\mathbf{X}_n$  associated to a set of cable lengths  $\{L_{0_n}^1, L_{0_n}^2, \dots, L_{0_n}^n\}$ . The Young modulus  $E_i$  for each cable is supposed to lie in the range  $[E_i, \bar{E}_i]$ . According to the variation of the  $E_i$ s the real pose of the CDPR will be  $\mathbf{X}_r$  and we have to solve the following optimization problem: *Find Min/Max* of  $(X_r^i - X_n^i)$  under the constraints  $\mathcal{H}(\mathbf{X}_r) = 0$  and all  $E_i \in [E_i, \bar{E}_i]$  with the guarantee of finding the global minimum and maximum  $\Delta X_m^i, \Delta X_M^i$  up to an arbitrary accuracy  $\alpha$  (the returned value differing from the global extrema by at most  $\alpha$ ). As this is a difficult problem we will rely on a 2 steps approach: first we will determine the minimum and maximum obtained for extremal values of the  $E_i$  and then we will check if a better extremum may be obtained for  $E_i$  not equal to  $\underline{E}_i, \bar{E}_i$ .

#### A. Minimum and maximum positioning error candidates

We have therefore to determine the values of the elements of  $\Delta \mathbf{X} = \mathbf{X}_r - \mathbf{X}_n$  for all possible combinations of the  $E_i$  involving their extremal values. The *status code* of a combination  $j$  is a pair constituted of  $\mathbf{S}_j$ , a  $n$ -dimensional list whose elements  $i$ -th is 1 if  $E_i = \bar{E}_i$  and -1 if  $E_i = \underline{E}_i$  and an associated pose  $\mathbf{X}_j$ . If the pose associated to this combination is not yet known, then a flag  $\mathcal{U}_j$  is set in the status code. The cables lengths for reaching  $\mathbf{X}_n$  have been obtained by solving the inverse kinematic problem, assuming known value  $\bar{E}_i^n$  for the  $E_i$  and we will assume that we have

$E_i^n = \overline{E_i}$ ], although this assumption is not restrictive, as will be seen later on.

When starting all combinations have this flag set in their status code except the first combination with  $\mathbf{S}_1 = \{1, 1, \dots, 1\}$  and  $\mathbf{X}_1 = \mathbf{X}_n$ . A key element for finding the  $\mathbf{X}_j$  of all combinations is an algorithm  $\mathcal{A}$  that find the unknown  $\mathbf{X}_j$  of a combination  $j$  as soon as there is a combination  $k$  with known  $\mathbf{X}_k$  with  $\mathbf{S}_k$  that differs from  $\mathbf{S}_j$  only by a single element numbered  $l$  (this occurs for example for the combination with  $\mathbf{S}_2 = \{-1, 1, 1, \dots, 1\}$ , which differs from  $\mathbf{S}_1$  only by its first element). The algorithm  $\mathcal{A}(\mathbf{X}_k)$  is based on a continuation process that starts with  $E_l = \overline{E_l}$ :

- we set  $E_l = \overline{E_l} - \epsilon$ , where  $\epsilon$  is an arbitrary positive number, lower or equal to  $\overline{E_l} - \underline{E_l}$ , and we use the Newton scheme with  $\mathbf{X}_k$  as initial guess for determining the robot pose. for the new  $E_l$ . To guarantee the convergence of the Newton method and the uniqueness of the solution in the vicinity of  $\mathbf{X}_k$  we check if the Kantorovitch theorem conditions are satisfied [19]. If this is the case the uniqueness of the solution and the convergence of the Newton scheme are guaranteed, otherwise we divide  $\epsilon$  by 2 and check again the Kantorovitch conditions. Convergence should be guaranteed for some  $\epsilon$  to obtain the pose  $\mathbf{X}_j$  for the current  $E_l$
- the process is repeated until we get  $E_l = \underline{E_l}$ .

Note that this process may also be used if one or several  $E_i^n$  are not equal to  $\overline{E_i}$  or  $\underline{E_i}$ : we will change each  $E_i$  in turn to get them to the closest  $\overline{E_i}$ ,  $\underline{E_i}$  to end up with a combination that has only extremal  $E_i$ .

We may now describe the algorithm we are using for finding the pose for all combinations. The status code of all the combinations is described in a list  $\mathcal{L}$  of size  $h$ , whose  $i$ -th element is the status code of combination  $i$  and we use an index  $k$  initially set to 1:

- 1) if  $k = h + 1$ , then exit
- 2) if  $\mathcal{U}_j = 0$ , then  $k = k + 1$ , goto step 1
- 3) if there is a  $m$  such that  $\mathbf{S}_m$  differs from  $\mathbf{S}_k$  by a single element and such that  $\mathcal{U}_m = 0$ , then  $\mathbf{X}_k = \mathcal{A}(\mathbf{X}_m)$ . Set  $k = 1$ , goto step 1

This algorithm just build up incrementally on a combination  $\mathbf{S}_m$  with known pose to determine the pose for all the combinations.

After this step we will have obtained a lower bound  $\Delta\hat{X}_i^M$  for the maximum and an upper bound  $\Delta\hat{X}_i^m$  for the minimum of each element  $i$  of  $\Delta\mathbf{X}$ .

## V. CHECKING STEP

Our ultimate goals are to determine the **global** minimum and maximum of  $\Delta\mathbf{X}$  with an accuracy  $\alpha$  but also to have a method that is extensible for managing all the uncertainty sources (such as uncertainties on the location of the  $A, B$ ) and provide a worst case analysis. One of the numerical methods that allows for determining global extremum is *interval analysis* that is especially convenient in our case as all uncertainties are bounded.

Using the data of the previous section we have already an estimate of the minimum and maximum of the positioning errors under the assumption that the extremum is obtained when the  $E_i$  have all an extremal value. But we have to check if if the global maximum and minimum may be reached for values of the  $E_i$  that are not all extremal.

For that purpose we set in turn each element  $X_i$  either to  $\Delta\hat{X}_i^m - \alpha$  or to  $\Delta\hat{X}_i^M + \alpha$ , while the other elements  $X_j$  will be assigned an interval value of  $[\Delta\hat{X}_j^m, \Delta\hat{X}_j^M]$ . Our purpose here is to detect if there are values for the  $E_i$  in  $[\underline{E_i}, \overline{E_i}]$  such that  $\Delta X_i$  exceed  $\Delta\hat{X}_j^m, \Delta\hat{X}_j^M$ . For that purpose we use an interval analysis-based approach that relies heavily on the specific properties of the Irvine equations [20]. For example it may be shown that the derivatives of  $x^r, z^r$  with respect to  $F_x, F_z$  have a constant sign if the upper bound of  $F_z$  is lower than  $\mu g L_0 / 2$  or the lower bound of  $F_z$  is greater than  $\mu g L_0 / 2$ . This implies that in that cases the interval evaluation of  $x^r, z^r$  will not be overestimated if  $L_0$  has a constant value, with a high consequence on the computation time of interval analysis-based algorithm.

If there is no location of the  $E_i$  with a better extremum this algorithm is relatively fast except when the  $E_i$  have values that are close to the extremal values that have led to  $\Delta\hat{X}_i^M, \Delta\hat{X}_i^m$ . But in that case we use the implicit function theorem to obtain the derivatives of the unknown function  $S(\mathbf{E})$  that provides the unknowns  $\mathbf{X}, F_x, F_z$ . Then the mean value theorem is used to find bounds  $S(\mathbf{E})$ , that are used to filter out the current intervals for these unknowns.

If values for the  $E_i$  are found such that  $\Delta\hat{X}_i^M + \alpha$  or  $\Delta\hat{X}_i^m - \alpha$  are reached, then we use a gradient-descent algorithm to obtain new value for  $\Delta\hat{X}_i^m$  or  $\Delta\hat{X}_i^M$  and the check step is repeated.

This approach requires to determine bounds for the unknowns  $F_x, F_z$  but the Irvine equations allows to establish safe bounds for these variables as presented in the Annex.

## VI. EXTENSIONS

In the previous sections we have addressed uncertainties in the  $E_i$  but the approach may deal with other uncertainties without changing its principle. For example we can use exactly the same algorithm for dealing with uncertainties in the  $L_0^i$  instead of the  $E_i$ . We may also as well manage uncertainties in both  $E_i$  and  $L_0^i$ . This increase the number of extremal cases to consider (we have  $2^n$  such cases if we consider  $n$  variables with uncertainties) but we will see in the example section that the complexity is still tractable.

An important aspect of this possible extension is to incorporate uncertainties in the  $E_i$  but use the possibility to manage interval values for the  $L_0$ . A box for the  $L_0$  will be mapped to a region in the operational workspace, meaning that by doing this calculation for several boxes we may check the positioning accuracy over a pre-defined operational workspace. For that purpose it will be required to somewhat modify the algorithm of section IV-A. Extremal points in that case are described by a n-uplet of  $E_i$  and a n-uplet of  $L_0$  and we consider that the nominal pose  $\mathbf{X}_n$  is the one obtained

for the n-uplet of  $\overline{E}_i$ . Initial values for the extremum of the positioning error will then be calculated as the difference between  $\mathbf{X}_n$  and the poses obtained for all combinations of  $E_i$  that include at least one  $\underline{E}_i$ . A similar change has to be made for the verification checking.

This extension has also the interest of allowing to manage simultaneously all the solutions of the inverse kinematics even for redundant CDPR i.e. calculating the worst case for the positioning errors. The algorithm and its extension will be illustrated in the next section.

## VII. EXAMPLE

We are considering a redundant planar 4-cables CDPR that lies in a vertical plane. The coordinates  $x, z$  in meters of its attachment points are  $A_1(-1, 1)$ ,  $A_2(1, 1)$ ,  $A_3(1, -1)$ ,  $A_4(-1, -1)$ , while the platform is a square with edge length 0.5, the center of mass of the platform being the center of the square. The Young modulus of the cable material is set either to  $5e^6$  Pa (typical for Nitrile),  $5e^9$  Pa (typical for Nylon) or  $1e^{11}$  (typical for Aramid), the cable diameter is 6 mm and  $\mu = 0.2219$  kg/m. The platform parameters are the  $x_C, z_C$  coordinates of the center of mass and the rotation angle  $\theta$  which is the angle between the  $x$  axis of the reference frame and of the mobile frame.

We choose as nominal pose  $x_C = z_C = -0.2$  and  $\theta = 0$  degrees. We use an inverse kinematics solver to obtain one solution for the cable lengths at this pose with  $L_0^1 = L_0^2 = 1.39387$  and  $L_0^3 = L_0^4 = 1.152159$  for  $E_i = 5e^6$ ,  $L_0^1 = L_0^2 = 1.6325$ ,  $L_0^3 = L_0^4 = 1.2907$  for  $E_i = 5e^9$  and  $L_0^1 = L_0^2 = 1.6327$ ,  $L_0^3 = L_0^4 = 1.29088$  for  $E_i = 1e^{11}$ . Note that if we have assumed ideal cable we will have got  $L_0^1 = L_0^2 = 1.63248277$ ,  $L_0^3 = L_0^4 = 1.29034879005$ . We then assume that because of the wear the Young modulus of the cable may decrease by 20%, leading to a range for the  $E_i$  respectively equal to  $[4e^6, 5e^6]$  Pa,  $[4e^9, 5e^9]$  and  $[8e^{10}, 1e^{11}]$ .

The initial estimations of the extremum obtained by using the algorithm presented in section IV-A, implemented in Maple, with a load of 1 kg, for two ranges for the  $E_i$  are presented in table I, where the three first columns represent the  $\Delta$ , while the following number are 1 if  $E_i = \overline{E}_i$ , -1 if  $E_i = \underline{E}_i$ . The computation time is 0.97 seconds in both cases.

$E$	$[4e^6, 5e^6]$	$[4e^9, 5e^9]$	$[8e^{10}, 1e^{11}]$	1	2	3	4
$\Delta x_C^m$	-0.03031	$-0.5e^{-4}$	$-0.2628e^{-5}$	1	-1	-1	1
$\Delta x_C^M$	0.03031	$0.51e^{-4}$	$0.2628e^{-5}$	-1	1	1	-1
$\Delta z_C^m$	-0.028	$-5.46e^{-5}$	$-0.29e^{-5}$	-1	-1	1	1
$\Delta z_C^M$	0.0182	$1.38e^{-5}$	$0.7e^{-6}$	1	1	-1	-1
$\Delta \theta_C^m$	-0.071039	$-0.808e^{-4}$	$-0.412e^{-5}$	1	-1	1	-1
$\Delta \theta_C^M$	0.071039	$0.808e^{-4}$	$-0.412e^{-5}$	-1	1	-1	1

TABLE I

EXTREMAL POSITIONING VARIATION (IN METER AND RADIAN) FOR EXTREMAL VALUE OF THE  $E_i$

We then set  $\alpha$  to  $1e-5$  for the first range and  $1e-9$  for the second one and use the algorithm presented in section V to

verify if the above result may be exceeded. The computation time for checking each of the 6 extrema is about 30 seconds.

We then set the platform mass to 100 kg. For  $E_i$  in the range  $[4e^9, 5e^9]$  we get  $\Delta x_C^m = -0.438$  cm,  $\Delta x_C^M = 0.438$  cm,  $\Delta z_C^m = -0.308$  cm,  $\Delta z_C^M = 0.234$  cm,  $\Delta \theta_C^m = -0.00714$  rd and  $\Delta \theta_C^M = 0.00714$  rd.

For  $E_i$  in the range  $[8e^{10}, 1e^{11}]$  we get  $\Delta x_C^m = -0.023$  cm,  $\Delta x_C^M = 0.023$  cm,  $\Delta z_C^m = -0.0157$  cm,  $\Delta z_C^M = 0.0119$  cm,  $\Delta \theta_C^m = -0.000358$  rd and  $\Delta \theta_C^M = 0.000358$  rd.

As may be seen from this examples change in the  $E_i$  have a very small effect on the positioning accuracy except if the cable are very elastic. A change on the Young modulus has also a small effect on the inverse kinematic solving. For example for a mass  $m=100$  kg and  $E_i = 1e^{11}$  we get a kinematic solution with  $L_0^1 = L_0^2 = 1.63118261912$  and  $L_0^3 = L_0^4 = 1.28950359$ . If we change  $E_i$  to  $0.8e^{11}$ , while keeping the same values of  $L_0^1, L_0^2$  obtained for  $E_i = 1e^{11}$ , we get  $L_0^3 = L_0^4 = 1.2895727468$  and therefore a minimal change. On the other hand we get significant changes in the cable tensions: for example for  $E_i = 1e^{11}$  the tensions are  $\tau_1 = \tau_2 = 2000.25883$ N,  $\tau_3 = \tau_4 = 1854.447216270$ N, while for  $E_i = 0.8e^{11}$  we have  $\tau_1 = \tau_2 = 801.41032518$ N,  $\tau_3 = \tau_4 = 1362.4796774$ . A good point for safety must be noticed: if we use the inverse kinematics solutions obtained for the upper bound of the Young modulus, then the cable tension will decrease if the Young modulus is lower than this upper bound.

We then consider having uncertainties in the  $L_0^i$  instead of the  $E_i$ . We assume that the  $L_0^i$  may have a value that differs from the nominal value  $L_0^n$  by  $\pm \Delta L_0$ . We set  $E_i = 5e^6$ ,  $m=1$ kg and table II presents the result for  $\Delta L_0=0.01$  m and 0.02m. In these tables the two first columns represents the  $\Delta$ , while the other numbers are 1 if  $L_0^i = L_0^n + \Delta L_0$  and -1 if  $L_0^i = L_0^n - \Delta L_0$

$\Delta L_0$	$\pm 0.01$	$\pm 0.02$	1	2	3	4
$\Delta x_C^m$	-0.016398	-0.03278	-1	1	1	-1
$\Delta x_C^M$	0.016398	0.03278	1	-1	-1	1
$\Delta z_C^m$	-0.01287	-0.0257	1	1	-1	-1
$\Delta z_C^M$	0.0182862	0.02573	-1	-1	1	1
$\Delta \theta_C^m$	-0.03833	-0.077	-1	1	-1	1
$\Delta \theta_C^M$	0.03833	0.077	1	-1	1	-1

TABLE II

EXTREMAL POSITIONING VARIATION (IN METER AND RADIAN) FOR EXTREMAL VALUE OF THE  $L_0^i$  FOR  $\Delta L_0 = \pm 0.01, \pm 0.02$ m,  $m=1$ KG AND  $E_i = 5e^6$  Pa.

If we set now  $m=100$ kg,  $E_i = 1e^{11}$ Pa, then we get the results presented in table III.

The analysis of this section shows clearly that in term of positioning accuracy the influence of uncertainty in the elasticity parameter has a marginal effect compared to uncertainties in cable lengths. On the other hand cable tensions may be severely impacted by these uncertainties.

We have mentioned in the extension section VI that the proposed algorithm allows one to check not only a pose but

$\Delta L_0$	$\pm 0.01$	$\pm 0.02$	1	2	3	4
$\Delta x_C^m$	-0.01923	-0.03845	-1	1	1	-1
$\Delta x_C^M$	0.01923	0.03845	1	-1	-1	1
$\Delta z_C^m$	-0.0118	-0.0236	1	1	-1	-1
$\Delta z_C^M$	0.011785	0.02355	-1	-1	1	1
$\Delta \theta_C^m$	-0.029273	-0.05855	-1	1	-1	1
$\Delta \theta_C^M$	0.029273	0.05855	1	-1	1	-1

TABLE III

EXTREMAL POSITIONING VARIATION (IN METER AND RADIAN) FOR EXTREMAL VALUE OF THE  $L_0^i$  FOR  $\Delta L_0 = \pm 0.01, \pm 0.02m, m = 100kg$  AND  $E_i = 1e^{11}Pa$ .

also a set of poses defined by a box for the  $L_0$ . As an example we have considered such a box defined by a range for all  $L_0^i$  equal to  $[L_{0_i}^n, [L_{0_i}^n - 0.1]]$ , where  $L_{0_i}^n$  is the cable lengths used for the pose  $(0, -0.2, 0)$ . We assume a mass of 1 kg and a range  $[4e^6, 5e^6]$  for the  $E_i$ . The results is that the extrema presented in table I are still valid.

### VIII. CONCLUSION

The algorithm proposed in this paper is generic for evaluating the effect of parameter uncertainties in CDPR at a given pose with a possible extension for checking the maximal positioning error over a whole workspace. The analysis of a planar and redundant CDPR has shown that errors in the evaluation of the Young modulus of the cable material has a marginal influence on the inverse kinematic solution and on the positioning errors, compared to errors generated by uncertainties on the cable lengths. On the other hand the elasticity has a strong influence on the cable tensions. If these results were confirmed over the whole workspace and for the general case of 6 d.o.f. CDPR, then this suggest that it will make sense of using a simplified Irvine model, assuming infinite value for the Young modulus and then correcting for the influence of elasticity by using a continuation approach (as the Irvine model is continuous in terms of the  $E, \mu$  parameters).

The proposed algorithm has the advantage to provide an estimation of the **global** extremal positioning errors with an arbitrary accuracy. But this guarantee has a cost in term of computation time, especially in the verification step. Improving the computation time of this step (e.g. by using the first and second order optimality condition) and applying the algorithm for CDPR with 6 d.o.f, possibly redundant, are our next objectives.

### IX. ANNEX

The purpose of this annex is to show that being given the pose of a CDPR and consequently the location of its attachment points in the cable plane, it is then possible to determine lower and upper bounds for the  $F_x, F_z$ . The calculation of these bounds is also valid for a set of poses that are constrained to lie within a bounded domain.

#### A. Finding bounds for $F_z$

By looking at the Irvine equations 2 it is easy to see that we will get  $z^r = 0$  for  $F_z = \mu g L_0 / 2$  and that  $z^r < (>) 0$  if  $F_z < (>) \mu g L_0 / 2$ .

Let us assume that  $z^r$  is negative (or equivalently that  $F_z < \mu g L_0 / 2$ ). Equation (2) may be written as  $z^r = B + A$  with  $A = (\sqrt{F_x^2 + F_z^2} - \sqrt{F_x^2 + (F_z - \mu g L_0)^2}) / (\mu g)$  that is negative and  $B = F_z L_0 / (EA_0) - \mu g L_0 / 2$ . Hence we have  $z^r = B - \epsilon$  with  $\epsilon > 0$  and  $B = z^r + \epsilon > z^r$  which leads to

$$F_z > \frac{EA_0 z^r}{L_0} + \frac{\mu g L_0}{2}$$

and  $EA_0 z^r / L_0 + \mu g L_0 / 2$  is a lower bound for  $F_z$ . Note that we have already the upper bound  $\mu g L_0 / 2$  for  $F_z$  but we may improve this bound. Indeed we have

$$\frac{\sqrt{F_x^2 + (F_z - \mu g L_0)^2} \leq \sqrt{F_x^2 + F_z^2} + \sqrt{2\mu g L_0 (\mu g L_0 / 2 - F_z)}$$

which leads to

$$\frac{\sqrt{F_x^2 + (F_z - \mu g L_0)^2} = \sqrt{F_x^2 + F_z^2} + \sqrt{2\mu g L_0 (\mu g L_0 / 2 - F_z)} - \epsilon$$

Consequently we have

$$z^r = B + \frac{(\epsilon - \sqrt{2\mu g L_0 (\mu g L_0 / 2 - F_z)})}{\mu g}$$

$$\frac{F_z}{EA_0} - \frac{\mu g L_0^2}{2} - \frac{\sqrt{2\mu g L_0 (\mu g L_0 / 2 - F_z)}}{\mu g} = z^r - \frac{\epsilon}{\mu g} < z^r$$

Let us define  $a = \sqrt{\mu g L_0 / 2 - F_z} > 0$  and consider the equation

$$H = -\frac{L_0 a^2}{EA_0} - \frac{\sqrt{2\mu g L_0}}{\mu g} a - z^r = 0$$

This equation has a negative root  $u_2$  and a positive root  $u_1$  with

$$u_1 = \frac{EA_0}{2L_0} \left( \sqrt{\frac{2L_0}{\mu g} - \frac{4L_0 z^r}{EA_0}} - \sqrt{\frac{2L_0}{\mu g}} \right)$$

that is independent from  $F_z$   $H$  is positive for  $a \in ]u_1, u_2[$  and as  $a$  must be positive  $H$  will be negative for  $a \geq u_1$ . This implies that  $H$  will be negative if  $\mu g L_0 / 2 - F_z > u_1^2$  or equivalently if  $F_z < \mu g L_0 / 2 - u_1^2$ . Therefore  $\mu g L_0 / 2 - u_1^2$  is an improved upper bound for  $F_z$  if we consider  $z^r$ .

Let us assume that  $z^r$  is positive (or equivalently that  $F_z > \mu g L_0 / 2$ ). In that case  $A$  is positive so that  $z^r = B + \epsilon$  with  $\epsilon > 0$ . Therefore we have  $B < z^r$  which leads to

$$F_z < \frac{EA_0 z^r}{L_0} + \frac{\mu g L_0}{2}$$

and consequently  $EA_0 z^r / L_0 + \mu g L_0 / 2$  is an upper bound of  $F_z$ , while  $\mu g L_0 / 2$  is a lower bound that can be improved. Consider that

$$\frac{\sqrt{F_x^2 + (F_z - \mu g L_0)^2} \geq \sqrt{F_x^2 + F_z^2} - \sqrt{2\mu g L_0 (F_z - \mu g L_0 / 2)}$$

so that  $A = (\sqrt{2\mu g L_0(F_z - \mu g L_0/2)} - \epsilon)/(\mu g)$ . so that  $G = B + \sqrt{2\mu g L_0} \sqrt{F_z - \mu g L_0/2} = z^r + \epsilon/(\mu g) > z_r$ . If  $a$  denote  $\sqrt{F_z - \mu g L_0/2}$  it is easy to show that  $G - z^r$  will be positive only if  $B$  is larger than the positive root  $u_2$  (that is equal to the previous  $u_1$ ) of  $G - z^r$  considered as a quadric polynomial in  $a$ . We get that

$$F_z > \frac{\mu g L_0}{2} + u_2^2$$

that will be minimal at  $z^r$ . If  $z_r$  has a negative lower bound and a positive upper bound, then the range for  $F_z$  will be obtained by taking as lower bound the one obtained for  $\underline{z_r}$  and as upper bound the one obtained for  $\overline{z_r}$ .

### B. Finding bounds for $F_x$

According to equation (1) we have

$$x^r = F_x(U + V)$$

with

$$U = L_0/(EA_0)$$

$$V = (\sinh^{-1}(F_z/F_x) - \sinh^{-1}((F_z - \mu g L_0)/F_x))/(\mu g)$$

If  $F_z < \mu g L_0/2$ , then  $V$  is negative so that we have  $x^r = F_x U + \epsilon$  with  $\epsilon > 0$  so that  $F_x U = x^r - \epsilon < x^r$ . The inequality  $F_x U < x^r$  leads to

$$F_x < \frac{EA_0 x^r}{L_0}$$

and an upper bound for  $F_x$  is therefore  $EA_0 \overline{x^r}/L_0$ . A natural lower bound for  $F_x$  is 0 but this bound may easily be improved. Indeed it is easy to show that  $\partial x^r / \partial F_x$  is positive so that if  $x^r(F_x)$  is lower than  $\underline{x^r}$ , then the lower bound for  $F_x$  is larger than  $\underline{F_x}$  and a better bound may be found efficiently by using a dichotomy process.

### REFERENCES

- [1] R. Babaghasabha, M. Khosravi, and H. Taghirad, "Adaptive robust control of fully constrained cable driven parallel robot," *Mechatronics*, vol. 25, pp. 27–36, 2015.
- [2] M. Korayem, M. Taherifar, and H. Tourajizadeh, "Compensating the flexibility uncertainties of a cable suspended robot using smc approach," *Robotica*, vol. 33, no. 3, pp. 578–598, 2015.
- [3] J. Sovizi *et al.*, "Wrench uncertainty quantification and reconfiguration analysis in loosely interconnected cooperative systems," *ASCE-ASME Journal of Risk and Uncertainty in Engineering Systems, Part B: Mechanical Engineering*, vol. 4, no. 2, 2017.
- [4] F. Thomas *et al.*, "Uncertainty model and singularities of 3-2-1 wire-based tracking systems," in *ARK, Caldes de Malavalla*, June 29- July 2, 2002, pp. 107–116.
- [5] A. Fortin-Côté, P. Cardou, and A. Campeau-Lecours, "Improving cable driven parallel robot accuracy through angular position sensors," in *IEEE Int. Conf. on Intelligent Robots and Systems (IROS)*, Daejeon, October, 9-14, 2016, pp. 4350–4355.
- [6] T. Dallej *et al.*, "Vision-based modeling and control of large dimension cable-driven parallel robot," in *IEEE Int. Conf. on Intelligent Robots and Systems (IROS)*, Vilamoura, October, 7-12, 2012, pp. 1581–1586.
- [7] H. M. Irvine, *Cable Structures*. MIT Press, 1981.
- [8] N. Riehl *et al.*, "On the determination of cable characteristics for large dimension cable-driven parallel mechanisms," in *IEEE Int. Conf. on Robotics and Automation*, Anchorage, May, 3-8, 2010, pp. 4709–4714.
- [9] M. Gouttefarde, D. Nguyen, and C. Baradat, "Kinostatics analysis of cable-driven parallel robots with consideration of sagging and pulleys," in *ARK, Ljubljana*, June 29- July 3, 2014, pp. 213–221.

- [10] S. Seriani, P. Gallina, and A. Wedler, "A modular cable robot for inspection and light manipulation on celestial bodies," *Acta Astronautica*, vol. 123, pp. 145–153, 2016.
- [11] K. Kozak *et al.*, "Static analysis of cable-driven manipulators with non-negligible cable mass," *IEEE Trans. on Robotics*, vol. 22, no. 3, pp. 425–433, June 2006.
- [12] H. Yuan, E. Courteille, and D. Deblaise, "Static and dynamic stiffness analyses of cable-driven parallel robots with non-negligible cable mass and elasticity," *Mechanism and Machine Theory*, vol. 85, pp. 64–81, March 2015.
- [13] J.-P. Merlet, "An experimental investigation of extra measurements for solving the direct kinematics of cable-driven parallel robots," in *IEEE Int. Conf. on Robotics and Automation*, Brisbane, 2018.
- [14] J. Kamman and R. Huston, "Multibody dynamics modeling of variable length cable systems," *Multibody System Dynamics*, vol. 5, no. 3, pp. 211–221, 2001.
- [15] J.-P. Merlet, "A generic numerical continuation scheme for solving the direct kinematics of cable-driven parallel robot with deformable cables," in *IEEE Int. Conf. on Intelligent Robots and Systems (IROS)*, Daejeon, October, 9-14, 2016. [Online]. Available:
- [16] S. Ghoreishi *et al.*, "Analytical modeling of synthetic fiber rope. part II: a linear elastic model for 1+6 fibrous structure," *Int. J. of Solids and Structures*, pp. 2943–2966, 2007.
- [17] W. Samuel *et al.*, "Synthetic mooring rope for marine renewable energy applications," *Renewable energy*, vol. 83, pp. 1268–1278, November 2015.
- [18] W. Wu and X. Cao, "Mechanics model and its equation of wire rope based on elastic thin rod theory," *International Journal of Solids and Structures*, vol. 102-103, pp. 21 – 29, 2016.
- [19] R. Tapia, "The Kantorovitch theorem for Newton's method," *American Mathematic Monthly*, vol. 78, no. 1.ea, pp. 389–392, 1971.
- [20] J.-P. Merlet, "Some properties of the Irvine cable model and their use for the kinematic analysis of cable-driven parallel robots," *Mechanism and Machine Theory*, vol. 135, pp. 271 – 280, 2019.